

“FUNDAMENTALS, APERTURE PROBES AND APPLICATIONS OF  
SCANNING NEAR-FIELD OPTICAL MICROSCOPY”

A PROJECT SUBMITTED TO  
**NIRMA UNIVERSITY**

In partial fulfillment of the requirements for the degree of

**Bachelor of Pharmacy**

**BY**

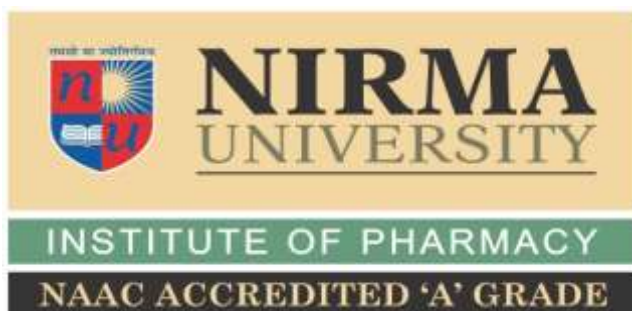
**MILI J. PATEL (16BPH056)**

**Semester VII**

**UNDER THE GUIDANCE OF**

**DR. CHARMY S. KOTHARI**

**(Guide)**



**INSTITUTE OF PHARMACY  
NIRMA UNIVERSITY  
SARKHEJ-GANDHINAGAR HIGHWAY  
AHMEDABAD-382481  
GUJARAT, INDIA**

**APRIL 2020**

CERTIFICATE

*This is to certify that "FUNDAMENTALS, APERTURE PROBES AND APPLICATIONS OF SCANNING NEAR-FIELD OPTICAL MICROSCOPY" is the bonafide work carried out by MILI J. PATEL (16BPH056), B.Pharm semester VIII under our guidance and supervision in the Institute of Pharmacy, Nirma University, Ahmedabad during the academic year 2019-2020. This work is up to my satisfaction.*

Guide:



Dr. Charmy S. Kothari  
M.Pharm., Ph.D.,  
Associate professor  
Department of pharmaceutical analysis  
Institute of pharmacy,  
Nirma University



Prof. Priti J. Mehta  
M.Pharm., Ph.D.,  
Head, Department of Pharmaceutical analysis,  
Institute of Pharmacy,  
Nirma University



20/07/2020

Prof. Manjunath Ghate  
M.Pharm., Ph.D.,  
Director,  
Institute of Pharmacy  
Nirma university

Date: 20/07/2020

CERTIFICATE OF SIMILARITY OF WORK

*This is to undertake the B.Pharm. Project work entitled "FUNDAMENTALS, APERTURE PROBES AND APPLICATIONS OF SCANNING NEAR-FIELD OPTICAL MICROSCOPY" Submitted by MILI J. PATEL (16BPH056), B.Pharm. Semester VIII is a bonafide review/research work carried out by me at the Institute of Pharmacy, Nirma University under the guidance of "DR. CHARMY S KOTHARI". I am aware about the rules and regulations of Plagiarism policy of Nirma University, Ahmedabad. According to that, the review/research work carried out by me is not reported anywhere as per best of my Knowledge.*



MILI J. PATEL (16BPH056),

Institute of Pharmacy

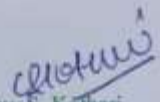
Nirma University

Sarkhej - Gandhinagar Highway

Ahmedabad-382481

Gujarat, India

Guide:



Dr. Charmy S. Kothari

M. Pharm., Ph.D.,

Associate professor,

Department of pharmaceutical analysis,

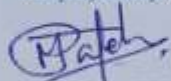
Institute of Pharmacy,

Nirma University

Date 20/7/2020

DECLARATION

I, MILI J. PATEL, (16BPH056), student of VIII<sup>th</sup> Semester of B.Pharm at Institute of Pharmacy, Nirma University, hereby declare that my project entitled "FUNDAMENTALS, APERTURE PROBES AND APPLICATIONS OF SCANNING NEAR-FIELD OPTICAL MICROSCOPY" is a result of culmination of my sincere efforts. I declare that the submitted project is done solely by me and to the best of my knowledge, no such work is done by any other person for the award of degree or diploma or for any other means. I also declare that all the information was collected from various primary sources (journals, patents, etc.) has been duly acknowledged in this project report.



MILI J. PATEL (16BPH056),

Institute of Pharmacy  
Nirma University  
Sarkhej - Gandhinagar Highway  
Ahmedabad-382481  
Gujarat, India

Date: 20/07/2020

### ACKNOWLEDGEMENT

I would like to take the opportunity firstly to thank Almighty for his constant shower of blessings in all my endeavors...

I would like to express my sincere thanks to all those concerned with my thesis as "FUNDAMENTALS, APERTURE PROBES AND APPLICATIONS OF SCANNING NEAR-FIELD OPTICAL MICROSCOPY". Also to all those who directly or indirectly assisted me in the completion of my thesis work. Secondly I would like to thank my parents and guardian for their timely support and their absolute love for me. Their guidance and care because of which reaching to this stage of life wouldn't be possible.

In providing the fundamental picture to my thesis I would take this opportunity to express my heartily gratitude to my guide Associate professor, Department of pharmaceutical analysis, Institute of pharmacy, Nirma University to Dr. CHARMY S. KOTHARI.

Her timely guidance and support provided shape to this project because of which I am truly grateful.

Lastly I would thank Dr. MANJUNATH GHATE for providing a platform to showcase my talent regarding this thesis.



SR. NO	CONTENTS	PAGE NO
1.	INTRODUCTION	8
2.	APERTURE SNOM	11
	A) GENERAL SETUP	11
	B) ASSEMBLY OF NEAR-FIELD OPTICAL PROBE	13
3.	BASIC TECHNIQUES	16
4.	PROBE MICROSCOPY TECHNIQUE	19
5.	CHARACTERIZATION OF AMORPHOUS & CRYSTALLINE ROUGH SURFACE: PRINCIPLE & APPLICATION	20
6.	REDUCTION OF LIGHT THROUGH A SUB WAVELENGTH OPTICAL MICROSCOPY	23
	A) TRANSMISSION COEFFICIENT OF APERTURE PROBE	23
	B) AREA DISTRIBUTION	26
7.	TIP-SAMPLE INTERACTIVITY & IMAGE DEVELOPMENT	28
	CAN-TIP PROBE NSOM	31
8.	PROBE DESIGNS & ITS METHODS	33
9.	SNOM: FUNDAMENTALS OF NEWER METHODS & TECHNIQUES	37

10.	NSOM APPLICATIONS	38
	A) AMPLITUDE & PHASE CONTRAST	38
	B)FLUORESCENCE TOPOGRAPHY	41
	C) NEAR-FIELD RAMAN SPECTROSCOPY	43
	D)PULSED LASER ABLATION THROUGH SNOM TIPS	50
11.	PERSPECTIVES	52
12.	REFERENCES	54

ABSTRACT

We explain the basics of scanning optical near-field microscopy with aperture probes in this study. Aspects of light propagation in metal-coated, tapered optical fibers are considered after consideration of instrumentation and probe manufacturing. It involves propagation properties in the vicinity of sub wavelength apertures as well as field distributions. In addition, the process for the creation of optical objects near-field is studied with special emphasis on possible artifact sources. Selected applications, including amplitude and phase contrast imaging, fluorescence imaging, and Raman spectroscopy, as well as optical near-field desorption, were discussed to illustrate the prospects of the technique. Such examples show that scanning optical near-field microscopy is no longer an uncommon process, but has become a valuable tool.



## 1. INTRODUCTION

Nowadays, the leading position of science and technology is Near-field scanning optical microscopy (NSOM) due to its power of examination of scanning techniques. This NSOM is the eyes to the nano world's technology. Alongwith it the key parameters are of attentiveness in nanostructure such as their structure shape and size, molecular structure, its dynamic properties and chemical composition too. For investigation of these properties microscopes required should be of high temporal even with spectral resolution too. The classic optical microscope is exceptional in terms of analyzing the spectra and material exclusive. Nevertheless, current mechanisms and applied science are increasingly in need of tools that allow structures to be characterized, produced and manipulated as small as a few nanometers in length.. It is necessary to operate electron microscopes in vacuum, limiting their use in life sciences. SNOM incorporates classical optical microscopy's excellent spectroscopic and temporal selectivity that extends well into the sub-100 nm system. Nevertheless, the widespread use of SNOM has been jeopardized by technical problems for a long time. We have now focused on the point where SNOM is a strong surface analysis tool that is well understood technologically and theoretically. It is able to be applied to a wide range of physical, chemical and biological problems. A lens captures or photographs the emitted light, scattered in a way by the target.

As Fourier light field components are generated exponentially around the standard body, the lens becomes unable to absorb them. This influence results in the famous Abbé diffraction cap  $x = (2/ NA)$ , 7: here NA( numerical opening of the lens).

The optical confocalscanning microscopy, situated on a narrowly targeted light beam covers widescreen illumination, will raise this range cap marginally.

In this area, more development is still being made by special lighting and detection geometries, often in combination with non-linear effects including multi photon excitation; however, steps are small and no big break is being made.

The obligation to expand optical microscopy's capacity more than the divergence limit has given rise to the progression of many hypothetical structures capable of generating nanometer-resolution optical images. The sample is positioned over a hemisphere substrate in the most general light detection arrangement, enabling all radiation from the sample touch region to be detected in the faraway area.



ig1

*Different types of scanning near-field optical microscopes: (a) aperture SNOM with angular resolved detection, (b) apertureless configuration, and (c) scanning tunneling optical microscope.*

*1. Field enhancement and gap-dependent resonance in a system of two opposing tip-to-tip Au nanotriangles Arvind Sundaramurthy et al., [Phys. Rev. B 72, 165409 \(2005\)](#)*

In this configuration, an external (far-field) illumination produces a highly confined optical range at the apex of a sharply pointed probe tip.<sup>9</sup> Therefore, the appropriate NFO signal must often be isolated from an enormous backdrop of radiation dispersed far-field.

## II. APERTURE NSOM

### A. *General setup*

Here focus on the NSOM aperture is mainly observed. These represents considerable developments in scenario of the importance of today's sub-100 nm system, also undoubtedly, aperture NSOM is actually the most commonly used and improved NFO technique. It can be demonstrated by the certainty that the aperture SNOM technique is used for all the materialistic devices available today.

Reasons for that circumstance are obvious in our view. With an general perspective, NSOM imagery is same as of confocal scanning excluding spot of light beam being compact. Of course, NSOM is a selective plane method, while confocal optical microscopy scanning can be benefitted and extended to thick samples requiring opticalmicroscopy.<sup>8,9</sup> However, the conventional optical microscopy requires all the processes of comparison, such as absorption, phasing and fluorescence comparison, to be more or less specifically transmitted. A light source with no context is very limited. It is opposed to the aperture less techniques where the focus of a very big, intense shaft spot is on a minute pointed-sharp peak.

Fluorescence studies being the best applications of NSOM, it is essential to have localized illumination as excess photobling of the sample must be prevented.

Extending current modern optical microscopes over a SNOM zooming level is straightforward and tempting. A standard SNOM configuration is viewed in Fig. A relatively long beam light is combined with an optical fiber at the far escape with an opening detector. The polarity and spectral light filters should be checked until they can be connected to the cable.

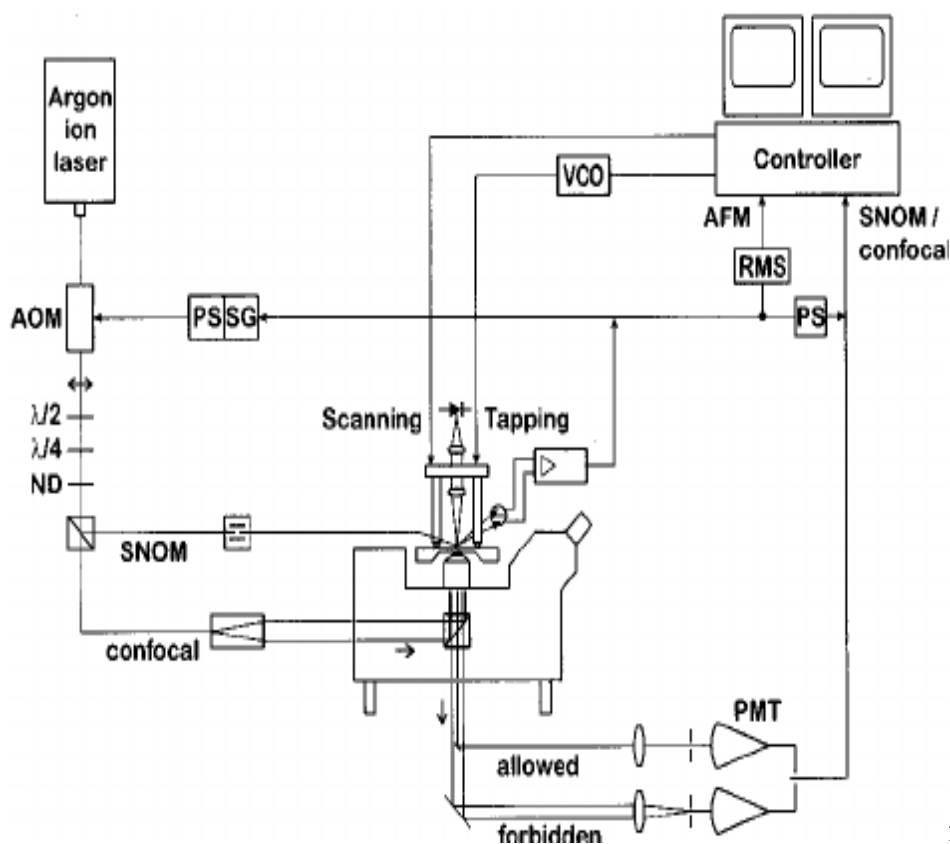


fig2

Standard SNOM setup consisting of (a) an illumination unit, (b) collection and redistribution unit, and (c) a detection module.

Field enhancement and gap-dependent resonance in a system of two opposing tip-to-tip Au nanotriangles Arvind Sundaramurthy et al., *Phys. Rev. B* 72, 165409 (2005)

A strongly gap width-dependent signal is required to calculate and monitor the gap-width between tip and sample. The fiber sample vibrates corresponding to sample top, ideally between 1-5 nm for one of its mechanical resonances. The magnitude and duration of this oscillation of a minute are tracked by an appropriate displacement sensor.

The resonant frequency is detached from the driving oscillator and triggering amplitude decreases and phase shifts. The cause of the shear force effect is not fully apparent.

Light produced through the aperture interacts locally with the test that may be excited fluorescence. Light emanating from the interaction zone must be obtained with maximum possible output, in any case. By using a plane parallel substratum, a proper benefit of an oil immersion objective is by absorb illumination that else may enter the detector by reflecting inside it. It is basically known as the 'forbidden light'.<sup>12,13,14,15</sup>.

Hemispheric substrates which gives a "solid immersion" may often utilize to catch the forbidden illumination in the case of mirror-based detection.

The captured beam of illumination is directed either through a crystal clear mirror to a visual and appropriate detector. Filters can be used to eliminate unnecessary components of the spectrum. Using a regular (inverted) optical microscope, light collection, redistribution and filtration are advantageous.

### ***B. Assembly of near-field optical probes***

Prominent attempts are being made to microfabricated NFO techniques.<sup>16</sup>

NFO group therefore yet depends greatly over tapered optical fibre-based aperture probes. Because fiber samples of adequate feature are costly and difficult for acquiring materialistic merchandize, manufacturing becomes of an interesting part.

The manufacturing method for fibre-oriented optical samples might categorized into two classes: (a) producing a plain cone with a sharp apex, and (b) ensuing aluminum covering non-transparent film to produce on taper walls.

There two methods are to prepare conical and tapering sharp apex: *(i) the process of heating and pulling, and (ii) chemical etching.*

- (i) *Heating and pulling* is a method dependent on generally heating using a CO<sub>2</sub> filament. The end peak shapes are greatly dependent on the temperature and duration of the heating and pulling.

In addition, flat appearance at the apex because to a final pulling cracks that allows the formation of an aperture while evaporation. Nonetheless, achieving a wide cone angle is difficult but not impossible; the transmission coefficient is correspondingly small for a given aperture.

(ii) *Chemical etching a second method* of optical fibers in HF solutions has become common since the invention of Turner's etching technique. The process is deployed on the assumption that the size of the meniscus is a mechanized fiber width that remains. CE enables greater amounts of samples to be processed more reproducibly in only one stage, thereby beginning the way to a lab-scale "mass production".

A particular benefit of Turner's system is that the conical angles are being modified. The aperture technique can therefore be generated with a correspondingly high transmission coefficient. The microscopic rigidness turns out to be a significant drawback of Turner's technique. It leads to sharpness and imperfections which interfere with the true NFO signals in the metal coating.

This issue was only addressed nearly by implementing a process called tube etching.<sup>19,20</sup> The fiber is not stripped in tube etching until it is dipped in HF.

The optical probe is created due to the vaporization of aluminium in both techniques. Because the evaporation occurs slightly from behind under an angle, the metal deposition rate over the peak is much lower than others. This geometric effect leads to an aperture at peak created by itself.

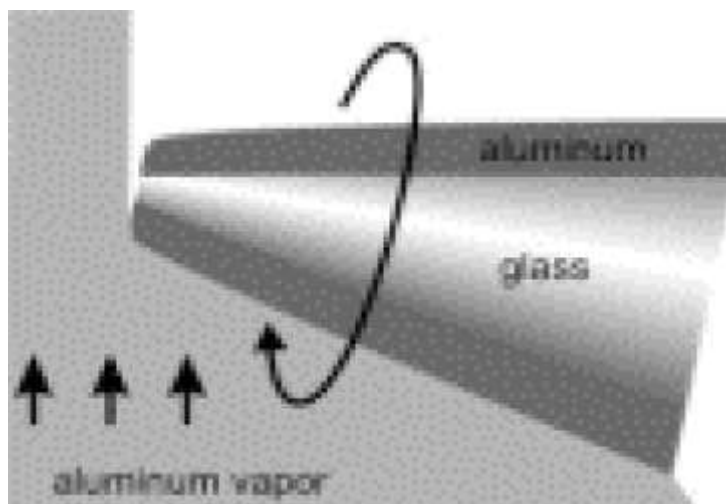


Fig 3

*Evaporation geometry of the aluminum coating process: evaporation takes place under an angle slightly from behind while the tip is rotating. The deposition rate of metal at the apex is much smaller than on the side walls.*

*Field enhancement and gap-dependent resonance in a system of two opposing tip-to-tip Au nanotriangles Arvind Sundaramurthy et al., [Phys. Rev. B 72, 165409 \(2005\)](#)*

It is clear that both tips possess an aluminum coating of comparably high quality. On Both tips can be observed at the aperture.

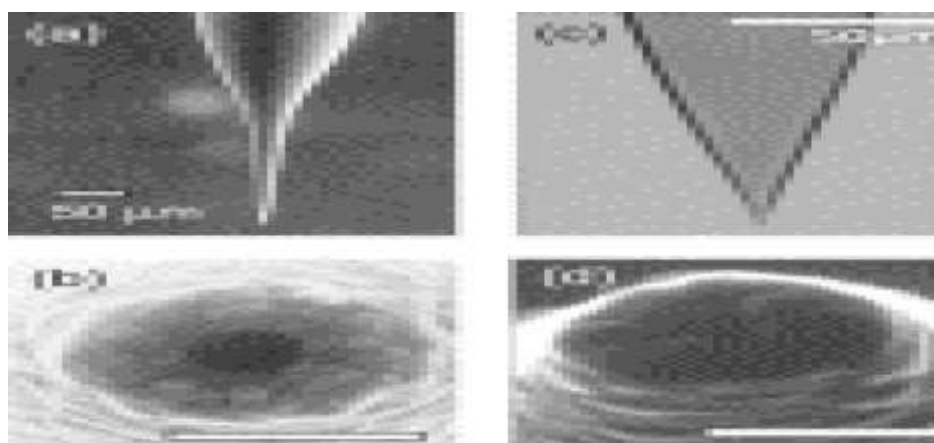


fig4(a)(b)(c)(d)

*Aluminum-coated aperture probes prepared by pulling (a),(b) and*

etching (c),(d): (a),(c) macroscopic shape, SEM and optical image. (b),(d) SEM close-up of the aperture region, scale bar corresponds to 300 nm.

Field enhancement and gap-dependent resonance in a system of two opposing tip-to-tip Au nanotriangles Arvind Sundaramurthy et al., *Phys. Rev. B* 72, 165409 (2005)

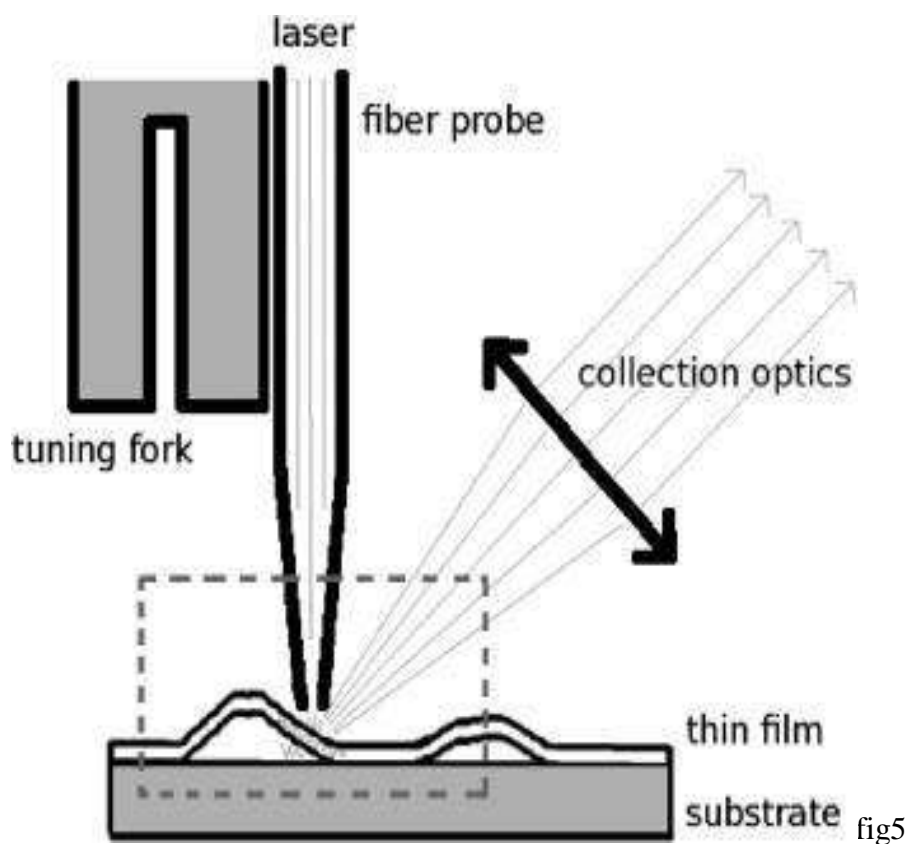
### **III. BASIC TECHNIQUES**

Basically, in all three axes each NSOM devices contains the feedback mechanisms for setting and measuring probe-sample distance, and optical devices for producing, directing, scattering and detecting light. A technique obtained from microscopy of atomic force is used to change the sensing intensity in the touch or non-contact test. Such adjustment makes the development of cantilevers from optical fibres, etc

Sources of light beam are of high potency because entire optical network is very low throughput. Spectrophotometers can also be used for applications involving spectroscopy. According to spectroscopy field of Raman technique we have a special family of measurements method called Tip enhanced Raman Scattering technique.

We name a wide variety of techniques having sharpened optical fiber as SPM probes as an aperture SNOM. Fiber may be used as a source, detector, or both on a nanoscale. This is normally made by a technique of pulling or etching. In commercial devices, to prevent the light from escaping past the aperture, fiber is attached to the feedback factor and examined near the sample. We may use the fiber probe as a origin or as a detector.





In the light manner or set manner, Aperture SNOM operates depending on the direction of light. Generally traditional optics establish the remainder of the optical path in order to optimize the light output.

Beam of illumination then passes through the probe and is reflected back as they exits the aperture (we can see it by eye for most of the probes).

Probes are scanned by pixels that form the final image. Continuous gap between the probe and the surface is usually established during sample movement.

### Apertureless NSOM and TERS

Due to large achievement of nanometer resolution, more trials and efforts are being made to reduce the size of the probe using tapered fiber technology at its highest possibilities that can be completed. The sample thereby serves to be transmitted light obtained from a far-field region. The calculation is normally achieved by the scanning of the metallic AFM probe on the limited distance from the determined sample surface. Specific lighting or illumination may be used with absolute reflection within the sample volume. Modulation of the tip-surface gap and the identification of the lock-in must be for the removal of the circumstances from other scatterers normally seen on the plain. The major advantages for this approach is not necessary for fiber technique and improved visibility but with possibilities having atleast detecting of single molecule.

On the contrary, for certain setups and sample geometries, the signal to noise ratio isn't optimal.

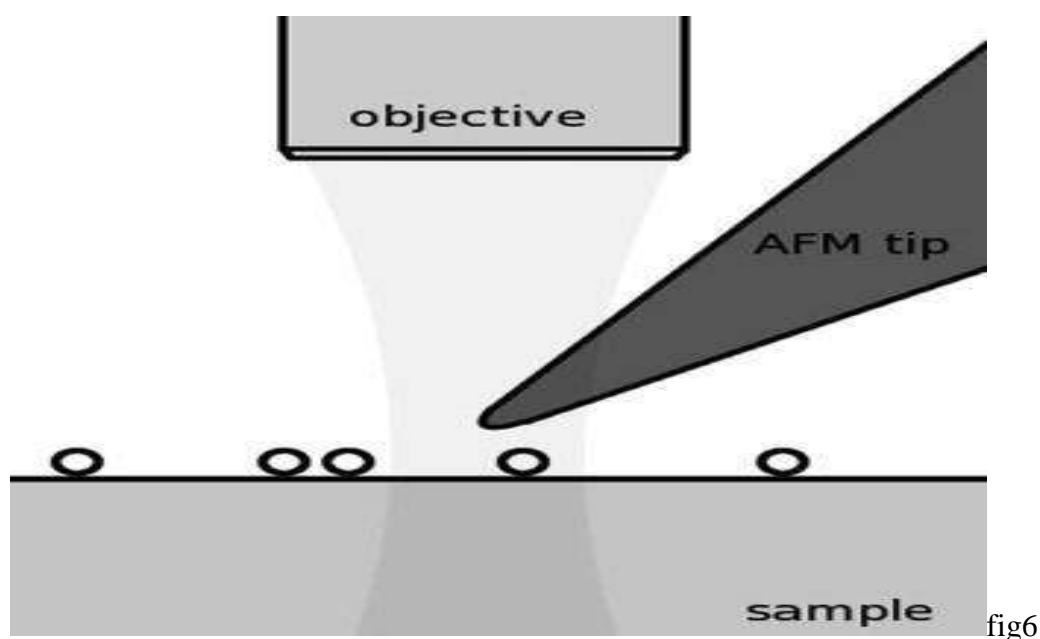


fig6

Electric field in this specific situation having its aperture peak with the enhancement and internment is well known to generate restricted Raman signal increasing for certain materials up to several orders of intensity. But this approach is not as commonly used as anticipated because of its entanglement and device cost. Local field development often depends heavily on peak properties, and its composition can be fairly complicated.

#### **IV. PROBE MICROSCOPY TECHNIQUES**

The scanning probe microscopy (SPM) provides topography with a surface atom or almost atomic resolution in its various formats and variations like tunneling microscopy scanning (STM). This is sample surface atomic or almost atomic resolution. A pointed peak is scanned near the sample area, and an image is obtained from the interactions between peak and surface area. Several different interactivity can be simultaneously imaged based on the method of operation, including physical properties along with information about configuration shape and fundamental structure.

Such methods are not commonly used for an analysis of surface pollution, largely due to the disadvantage of achieving chemical contrast and thus the chemical recognition of an individual atom. Nevertheless, recent chemical comparison has been demonstrated successfully in both STM and AFM. As addressed in newer advances in probe microscopy, including two specific techniques, *thermal microscopy scanning* and *acoustic microscopy scanning*, particle characterization and sub-surface characteristics.

## **V. CHARACTERIZATION OF AMORPHOUS AND CRYSTALLINE ROUGH SURFACE: PRINCIPLES AND APPLICATIONS**

### *Scanning optical microscopy*

Fundamental theory for scanning optical microscopy (SOM) is same as to Atomic Force Microscopy. Aperture Probe is used to calculate the object as a feedback instead of using surface force or tunneling current as the sensing signals. One of the most common NSOM technique is confocal optical microscopy scanning (CSOM). The theory of the CSOM technique is briefly discussed below.

### *Confocal scanning optical microscopy*

This theory is indicated in Fig 6.11. The rays of beam is centered by an objective by passing it through a pinhole. The light which is refracted again is placed on the pinhole by the substrate if sample surface is exactly positioned on the plane of focused lens. A detector in front of the pinhole collects the reflected light intensity (not shown in Figure 6.11). When the sample shifts at a pinhole it may be disturbed by its focus on the plane, and the intensity of the detector received decreases drastically.

Thus, one can change the location of the PZT holding the sample by using the observed strength as a feedback signal. Sample surface topography is given by the PZT location variation.

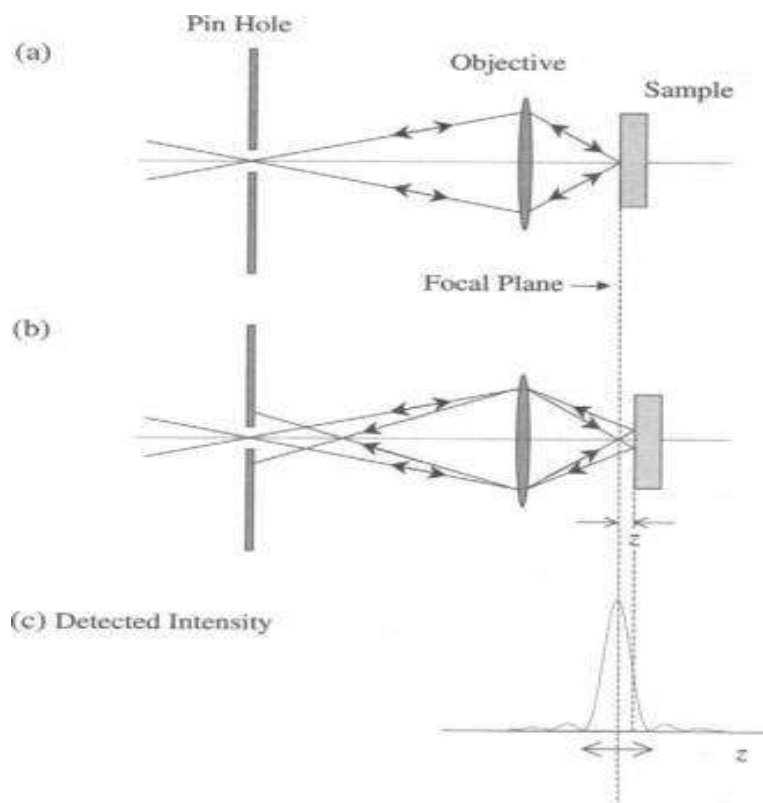


FIG 6.11

### Aperture probe near-field scanning optical microscopy (NSOM)

One technique for optical near-field microscopy is based on using apertures of sub wavelength in metal-coated optical samples and scanning a few nanometers above the sample. Diminishing the size of the aperture, however, would also significantly reduce the optical performance. As discussed in Section 11.4, for the subwavelength scales ( $d / \lambda \ll 1$ ) where  $d$  is the width of the aperture, the power output which is defined as the ratio of the total transmitted energy to the incident force over the aperture area (Shi and Hesselink, 2002). The aperture size is thus a constraint on the performance of these systems.

Choosing a suitable shape design for the apertures, such as C-shaped or bow-tie, will lead to major improvements in the power throughput. The light is centered on the

ridge at the aperture's exit surface for C-shaped apertures and provides a very powerful near-field. An enhancement of power efficiency of up to two or three orders of magnitude greater than square apertures can be achieved using these structures. For action, however, the optical spot sizes for these C-shaped structures are about 40–70 nm, limited by existing manufacturing technologies.

### Apertureless probe NSOM

An alternative technique for achieving higher resolution is dependent on the use of an optical microscopy (aNSOM) apertureless probe in near-field scanning. A very high concentration of light can be achieved by using a sharp metallic nanotip. Due to the sharpness of the tip apex, which defines the optical spot size, high resolution, with an optical spot size of less than 10 nm, was recorded using apertureless probes. The issue that comes up here is the background lighting.

The light coming from the source of laser light often illuminates a wide region around the sharp peak and interferes with the dispersed near-field from the sample. Given the very high concentration and enhancement of energy on the tip of the apertureless NSOM probe, background optical energy still exists and thus it is important to apply a modulation technique. The detector can detect only the near-field emission, which is a modulated signal, when using such a technique, and reject the unmodulated background light.

This effect is experimentally confirmed by imaging dielectric contrast of  $pn^+$ -nanostructured semiconductor, obtaining  $\lambda/100$  resolution at 10  $\mu\text{m}$  infrared wavelength.

## **VI. REDUCTION OF LIGHT THROUGH A SUBWAVELENGTH OPTICAL MICROSCOPY**

The APERTURE must incorporate pair of key effects to obtain best possible efficiency in an opening SNOM: I lowest possible dimension of the mark. Meanwhile (ii) illuminating potency will be maximum possible at the aperture.

Ultimately, the transmission of the illumination in the vicinity of the aperture should be as easy as possible for practical reasons.

Hence, the aperture probes is of primary importance for its recognition of the drawbacks and possibilities

### *A. Reflecting efficiency or ratio of aperture probes*

#### *1. The taper region*

The reflecting factor of the opening probe is determined by the light intensity combined in specific site separated into illuminating intensity released upon opening. A calculated estimation referred as fiber minus strength equal to reflective loss of 4 per cent.

In the far field also the power generated by the aperture is measured. However, the instantaneous electrical fields dominate light-matter interaction in almost all experimental circumstances.

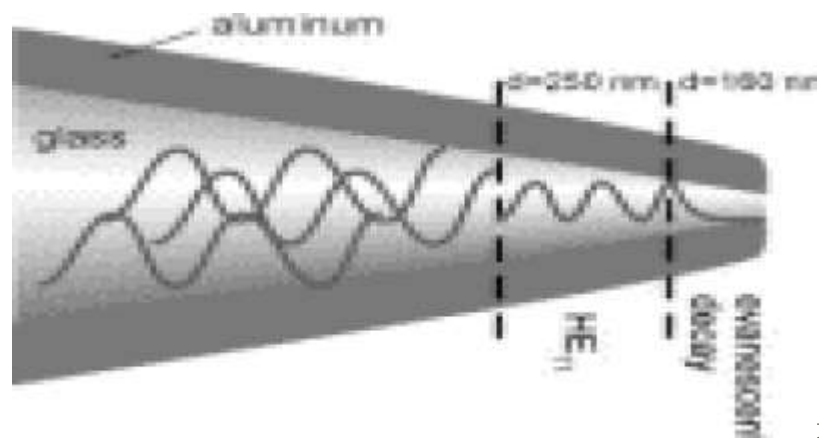


fig7

*Mode propagation in a tapered metal-coated optical fiber at a wavelength of 488 nm. Cutoff diameters taken from Ref. L. Novotny and C. Hafner, [Phys. Rev. E 50, 4094 \(1994\)](#). [ISI] [MEDLINE] [ChemPort] Field enhancement and gap-dependent resonance in a system of two opposing tip-to-tip Au nanotriangles Arvind Sundaramurthy et al., [Phys. Rev. B 72, 165409 \(2005\)](#)*

Along the comparison to power of HE11 mode, the light transmission coefficient until this point is primarily based on the power fraction found in cutoff modes. The magnitude of this factor will most probably be based on the taper's configuration.

Until now, this relation was poorly understood. Energy not included in the propagating modes is either mirrored in the waveguide or consumed in the metal surface, resulting in substantial metal heating

The HE11 mode also runs into cutoff, below an inner diameter of 160 nm.



## 2. The aperture

A particularly known subwavelength aperture Bethe / Bouwkamp model is important because it offers closed analytical exposure.

While the model does not accurately represent truth, the terms still contain the most characteristic features of a practical subwavelength aperture being spread near- and far-field.

In the Bethe / Bouwkamp model, it is predicted that a sub wavelength holes transmission coefficient will scale as  $a^4$ . As there is increase in the aperture diameter from 20 to 100 nm there is an increase in the transmission coefficient by 625.

To demonstrate this, we use Novotny measured transmission data at practical peak shape that are varying maximum conical sides at 10 and 20 nm aperture diameters.

The interpolated data points begin to diverge at greater taper angles. It is possibly because of the breakdown of the Bethe / Bouwkamp model.

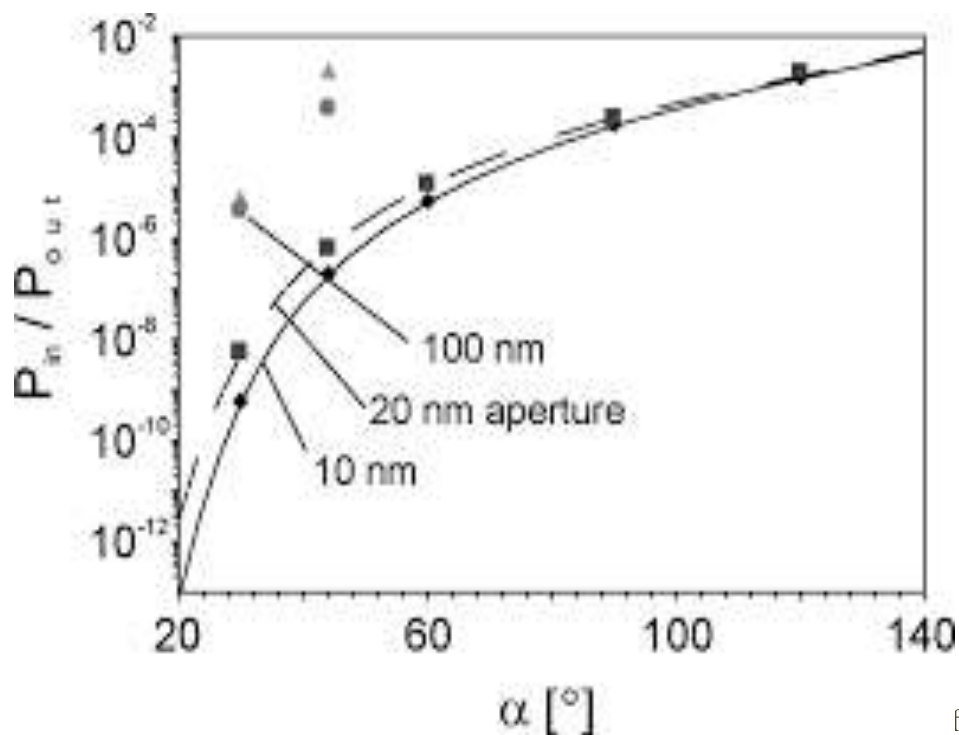


fig8

*Transmission coefficient of an aperture probe as a function of the full taper cone angle . Squares and rhombs: calculated values from Ref. 71 for a 20 and 10 nm diameter aperture, respectively. Circles and triangles: interpolated values determined by scaling the numerical data according to the Bethe/Bouwkamp  $a^4$  law by a factor of 104 and 54, respectively. This provides a simple approximation for the transmission coefficient of a 100 nm aperture.*

*Field enhancement and gap-dependent resonance in a system of two opposing tip-to-tip Au nanotriangles Arvind Sundaramurthy et al., [Phys. Rev. B 72, 165409 \(2005\)](#)*

Such numbers agree fairly with the coefficients of transmission stated in the literature and calculated in our laboratories..

**B. Area distribution**

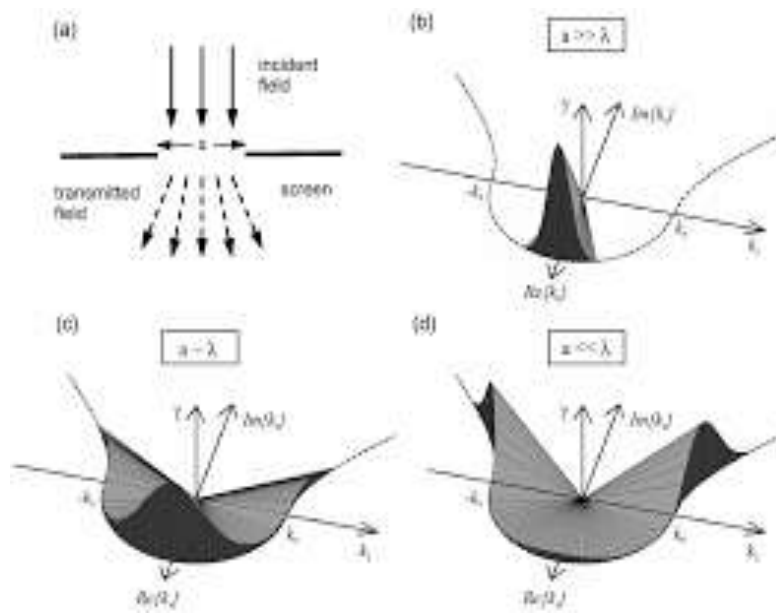


fig9

With the help of angular (Fourier) the character of this field can be understood in a better way. A pointed chromatic surface area (evanes too) can be provided by performing Fourier transformation on the screen plane. Here, components of transverse and longitudinal section of the  $k$  vector are  $k_z$  and  $k$ , respectively.

The purpose of this is not to provide the slit an accurate treatment of the scattering, but instead explain the SNOM aperture related to its physical phenomenon, and for that we should consider “ $k$ ” diagonal factor to be correct.

The evanescent signals makes up the field together describing for  $k$  and  $k_z$  the plane’s radiation properties. A sharp spectrum layers are represented in Figs for various aperture sizes. By (1) it is shown that two different forms of solutions for  $k_z$  are obtained depending on the magnitude of  $k_z$

The area part in the propagation direction that has an imaginary wave vector corresponds to an evanescent field.

If  $a \gg \lambda$ , then the incident field is very near to the angular distribution of the transmitted field, i.e propagation vector  $k_z \approx k_0$ ,  $k \approx 0$  [Figure] in the forward direction. (9)(b)].

As the size of the aperture is equal with the light intensity, the oblique concentration decrease, range widens also. Like consequence, area being transmitted is strongly diverging [Fig. (9)(c)]. The transmitted field angular spectrum contains a tiny sequence of definite dimensions and magnitude.

This implies that the transmitted field is heavily situated near the aperture and reduces distance quickly. Consequently, strength produced due to opening reduces, whereas the opening region shows closely restricted and enhanced fields.. Experimental proof for the presence of non-radiative fields near to a probe is the "forbidden light" emission also.

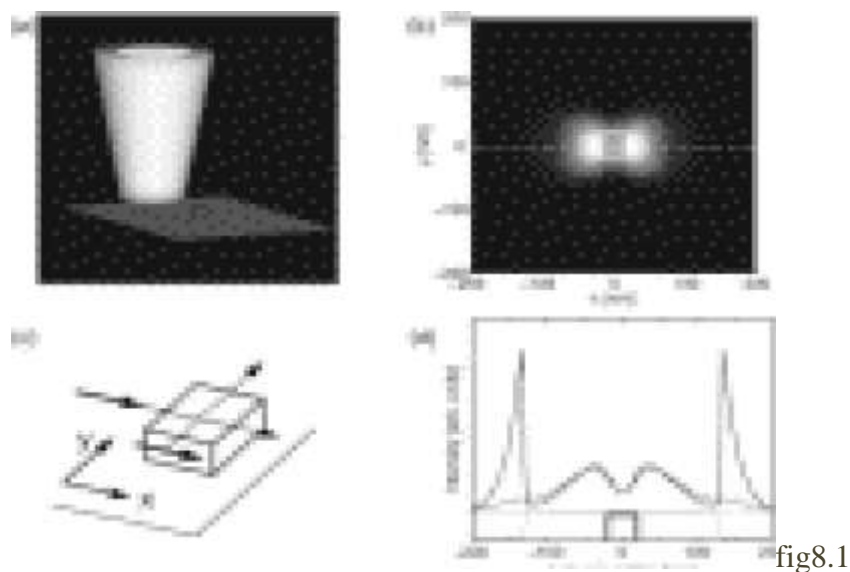
## **VII. TIP– SAMPLE INTERACTIVITY AND IMAGE DEVELOPMENT**

Consequently source of lights were confined as the importance of the SNOM. However the field is detected in most SNOM experiments at a far interval from the tip. The function of the evanescent illumination field is to convert into propagating field components that carries sample information.

To learn these complex contrast processes, accurate and flexible computational techniques are necessary. Most inherent troubling incentive for optical pictures are those which are a realistic experiment involves elements of quite several dimensions. The peak is also rather broad but very subtle in their contact with the test.

Thereby, as stated, the appropriate interaction of illuminating content occurs in the area of sample, the picture produced due to determination of changes in intensity at very far distance from the sample.

The conclusive merits of this matter is simulating NSOM tests may assist composite process having indefinite elements along with heavily confined preparations too. In addition, they let measurements for calculated area in a self-compatible way. Unfortunately, when high dielectric constant materials are in operation, the approach is ineffective.



*Simulation of image formation in near-field microscopy. (a) An accurate model for an SNOM experiment should include an aperture tip with a reasonably large extension, a sample, and an infinite substrate supporting the sample. (b) Total transmitted electric field intensity computed for the geometry depicted in (a). The sample is made of glass ( $n = 2$ ) and deposited on a glass substrate. The tip has a 50 nm opening with a 70 nm thick aluminum coating. The sample size is  $40 \times 40 \times 40$  nm<sup>3</sup>. The incident field is polarized in the  $x$  direction. To reproduce an experimental image, each pixel on this figure corresponds to a different calculation with a particular tip-sample position, the tip apex being kept at a constant height (2 nm) above the top sample surface. (c) The strong signals observed in (b) are related to depolarization fields created on the sample sides that are normal to the incident field. (d) Comparison of different scanning modes: constant height (dashed line) and constant gap (solid line) measured along the dashed line in (b). The corresponding tip motion is depicted at the bottom of the figure. When the sample is scanned in constant gap mode, i.e., when the tip motion follows the sample outline, the depolarization signal is much stronger as it is in constant height mode.*

*Field enhancement and gap-dependent resonance in a system of two opposing tip-to-tip Au nanotriangles Arvind Sundaramurthy et al., [Phys. Rev. B 72, 165409 \(2005\)](#)*

The findings obtained with this method are shown in figure 8. The current geometry representation is shown in Fig. 8.1(a), showing a fairly large peak needs to illustrate a tiny mirror blocks over sheet. In Fig8.1(b) we can see an image measured during a peakscanned over a circle. As in a practical experiment, the field transmitted via the device is measured.

The measured signal has a heavy asymmetry.

To understand this effect, it should be remembered that non-repolarization area  $E_d$  is generated so that the total field  $E_t = E_0 + E_d$  satisfies extremities state inflicted by Maxwell's equations. In this estimation it was chosen to polarize the illumination field  $E_0$  in the x direction. [Figure 8.1(c)].

On the contrarily, both vertical sides are not going along with the margin conditions on the x-polarized incident field. Infact, at this interface, the total electrical field will provide constant proportionality for preparations.

Hence, a strong depolarization field is created by the sample. Figure. (8.1)(b)

Here in SNOM, the contact within the field of incident and the sample sides occurs when the entire motion of the tip going upwards required for completing the sample outline. This corresponds to the prominent levels of depolarization.

On the other hand, our findings also show that to keep these objects under control a careful monitoring of the polarization of the illumination may provide another handle. The continuity in measurements of this device in particular, allow for distinction between topography artifact and actual near-field signal.

### CAN-tip probe NSOM

By taking advantage of both aperture probes' characteristics to block the background signal, and apertureless probes for high energy concentration and resolution, Frey et al. (2002) first proposed a new NSOM technique combining these two. A metal tip was introduced shaped on the aperture of a traditional fiber probe, known as the tip-on-aperture probe. In such a microscope, a sharp nanotip attached to the aperture concentrates the light that passes through the aperture.

A resolution of 16.1 nm was obtained in a more recent NSOM experiment using a C-shaped aperture, combined with a nanotip (CAN-Tip).

The nanotip, which functions as a metallic nanoantenna, spreads from the C-shaped nano aperture ridge (Cheng et al., 2011). While working at resonant frequency, the charges focus on the leaving area having C-shaped optic probe at ridge corners. Therefore, charges focused at the peak apex of the nanoantenna (electric fields are strongest at the object's sharpest features), which create an ultra-small optical spot of very high intensity. Figure 11.8 shows a schematic and SEM image of a fabricated CAN-Tip.

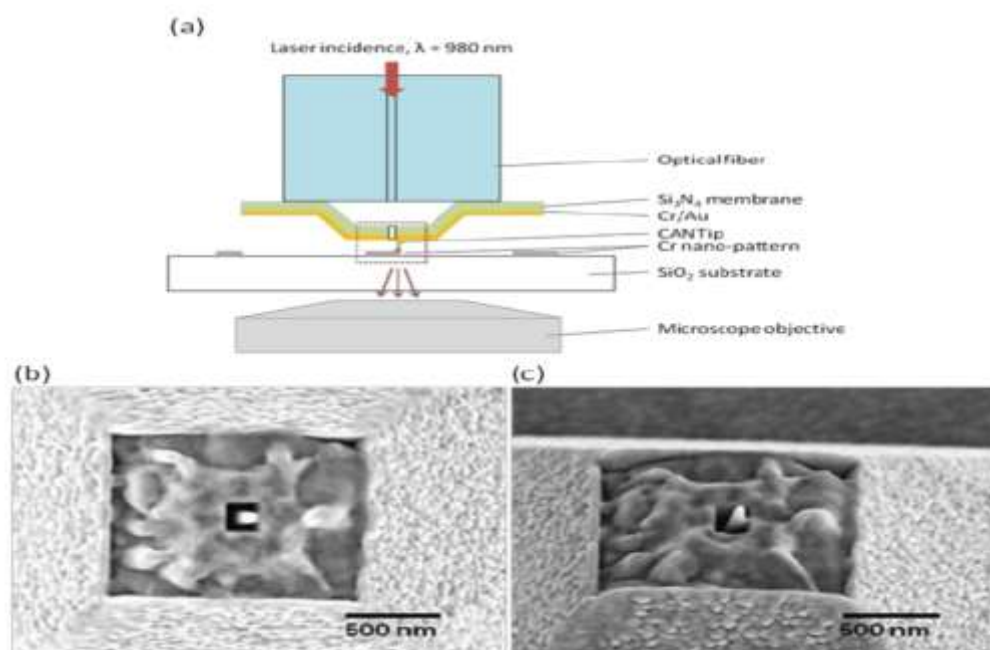


fig11.8

By designing the aperture and nanoantenna to resonate at a wavelength of 980 nm, Cheng et al. (2011) predicted high intensity (650 range) and high optical resolution ( $\sim$  range/60) for such a structure. Additionally, due to lack of background signal, no modulation technique is needed. Figure 11.9 shows the CAN-Tip NSOM response when scanning with a probe set at different distances from the center of the discs through three Cr nanodisks. This experiment showed an optical resolution of 16.1 nm.

By designing the aperture and nanoantenna to resonate at a wavelength of 980 nm, Cheng et al. (2011) predicted high intensity (650 range) and high optical resolution ( $\sim$  range/60) for such a structure.

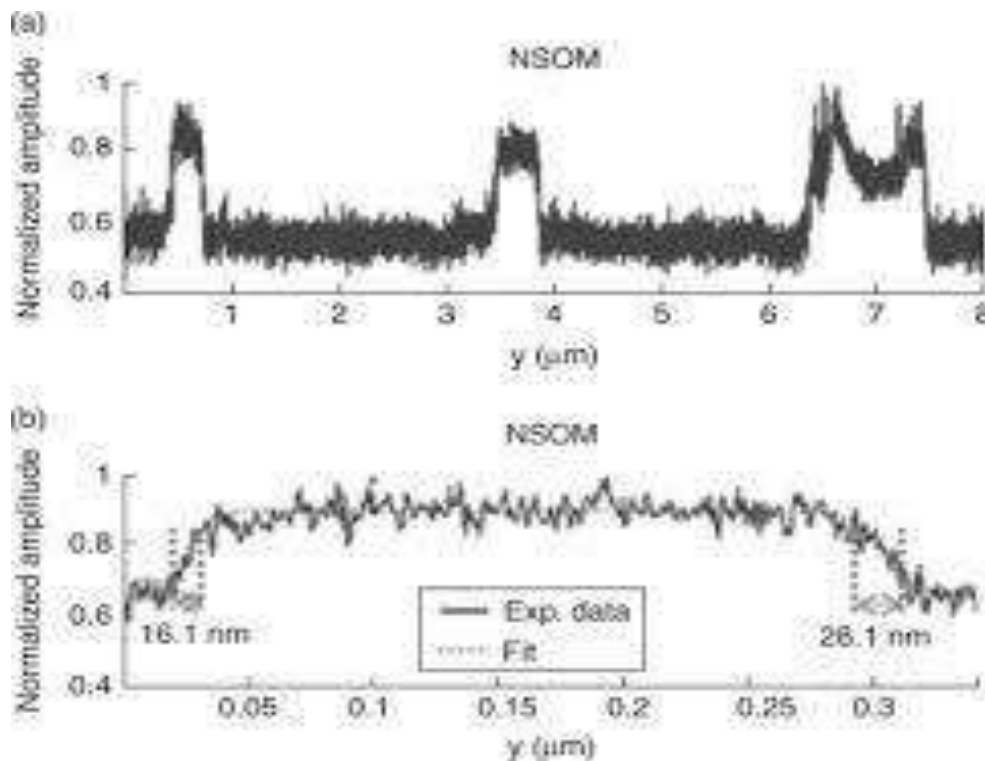


fig11.9



The overlapped running lines shows the data installed. The insufficient transition reveals an equal complete width of 16.1 nm at half Gaussian transition limit (FWHM) that demonstrates the CAN-Tip NSOM probe's 16.1 nm optical resolution.

This technique could potentially be used in a number of other apertures requiring major strength having nanoscale resolution.

The combination of SECM with other techniques, such as atomic force microscopy (AFM), near-field optical microscopy scanning (NSOM), and electrogenerated chemiluminescence (ECL), significantly increases the experiment's complexity and poses challenging issues in tip preparation. However, collecting information from two or more different techniques simultaneously and at the same location will significantly increase SECM's power (e.g., by supplying separate topographical or optical data during the SECM scan).

## **VIII. PROBE DESIGN**

The traditional AFM cantilever was combined with a means of localized thermometry using three methods.

### *1. Thermoelectric cantilevers*

The use of thermoelectric element AFM at the peak has been stated above.

Majumdar cemented a diamond shard to the junction in an attempt to upgrade the efficiency of a thermocouple peak to give better firmness and resoluteness and decreased thermal resistance.

The same party also describes how the thermo element pair cantilever at edge with high quality of A-frame AFM by depositing successive layers of various metals.Fish

et al. borrowed a scanning technique with near-field optical microscopes to build a gold-coated glass thermocouple that carries a Pt (Platinum) center. These kinds of research results in thermopile sensors being developed (including a heater) which are similar to a miniature calorimeter of heat flux.

## 2. Resistance thermometry

In 1994, the earliest collaborated SThM / Atomic Force Microscopy were described by Dinwiddie and Pylkki. Those were process wire made from Wollaston. This is a narrow platinum per five percent rhodium core having dense silver sheath. The overall wire dimension thereby exist approximately 75  $\mu\text{m}$ . The longitudinal wire shaped of "V" that acts as a thermometer for miniature resistance.

At the tip is attached a bead of epoxy resin to serve as an involuntary resistance and the silicon wafer sliver is fixed at the peak of the aperture to serve as a selective mirror used in the detection system. During the ending situation case, a greater ampere is transmitted through wire (sufficient to lift the probe's temperature above that of the surface). A voltaic crossover loop is used for controlling the power needed to assist the steady temperature difference between tip and sample.

Essentially, they are similar with calorimeter for strength satisfaction. Mills identify similar samples depositing the resistance factor near the tip of silicon nitride slurry same as traditional cantilever Atomic Force Microscopy.

These are to be used to measure the temperature distribution simultaneously with their topography in energized electronic devices. When the plane surface area is illuminated by IR sub wavelength rays, light insulation as a resultant can be used for obtaining infrared spectrum for sample.

Other designs for the resistant probes were published. Li and Gianchandani, for example, have manufactured SThM samples using silicone as a substratum in a method close to that of Mills, without taking advantage of the polyimide's mechanical

versatility to introduce a technique that removes the necessity for sample elimination or Silicone wafer termination.

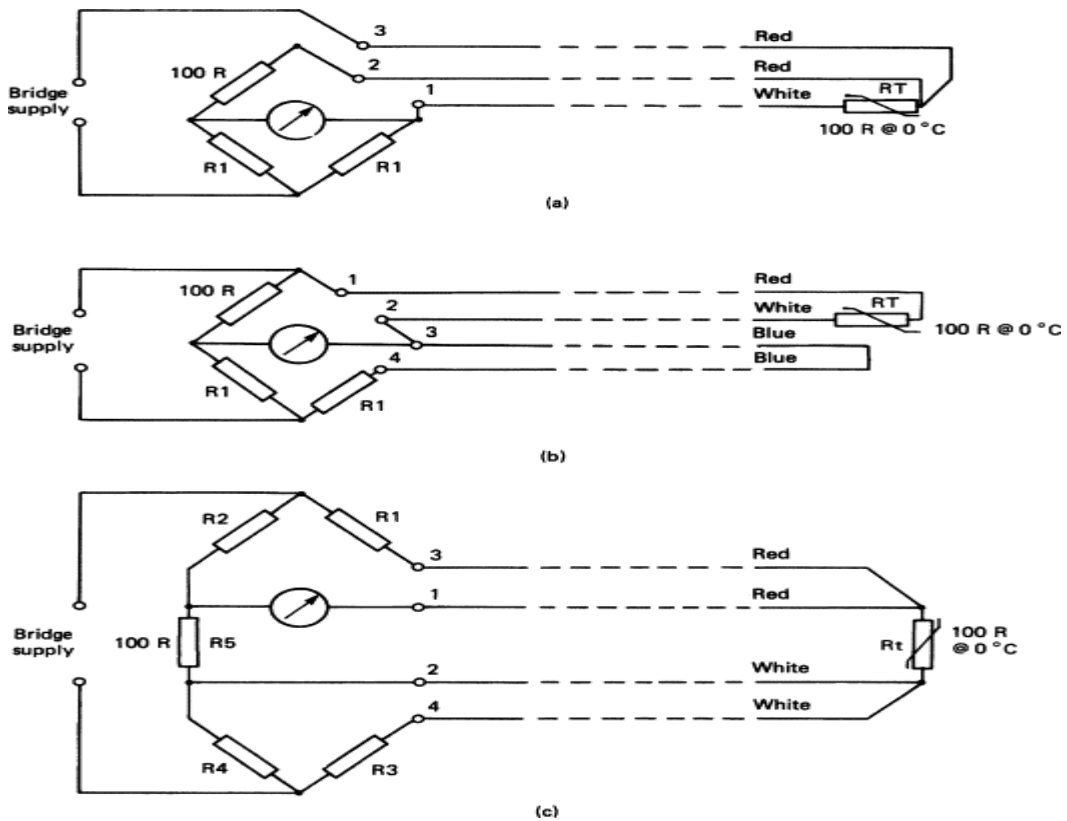
The using of silicone refers to a greater extent of thermal insulation than using the polyamide as a substratum, due to its conducting the insulation in triple dimension consistency is lower from silicone.

Such techniques were developed in a several positions.

Edinger describes a sensor composed of a nanometer-sized filament shaped at the end of a cantilever type of piezoresistive atomic force microscope.

The writers assert a spatial resolution having greater than twenty nanometer, a high sensitivity and rapid response time due to its low thermal mass.

fig12



### 3. *Bimetallic sensors*

Nakabeppu explains the usage of conventional AFM silicon nitride extruded cantilever samples made of tin or gold to track differences in spatial temperatures using a furnace for indium / tin oxide.

The diode component's thermal expansion prohibits the beam to bend.

The deflection detection system AFM optical lever leads this step.

Nakabeppu explains the usage of conventional AFM silicon nitride extruded cantilever samples made of tin or gold to track differences in spatial temperatures using a furnace for indium / tin oxide.

The diode component's thermal expansion prohibits the beam to bend.

The deflection detection system AFM optical lever leads this step.

This technique was useful to conduct insulation for thermal elements having capacity of substance collected at the end of a bimetallic cantilever picolitre. Arranging these kinds of equipment may have implementation like electronic "noses" heavily compassionate.

## **IX. SNOM: FUNDAMENTALS OF NEWER METHODS AND TECHNIQUES**

A new method for high-resolution imagery, optical microscopy near-field scanning (NSOM), has been developed. The principles governing this approach are discussed, explaining the technological challenges faced when constructing a working NSOM instrument. Two distinct methods for the manufacture of well defined, easily reproducible, subwavelength apertures are provided. A one-dimensional sample scan is given, and compared to a test pattern's scanning electron micrograph. A resolution of  $> 1,500 \text{ \AA}$  is estimated from this comparison (i.e.,  $\pi/3.6$ ), which represents a major step towards our ultimate target of  $500 \text{ \AA}$  resolution.

Apertures smaller than  $600 \text{ \AA}$  and signal-to-noise measurements indicate that fluorescent imagery should be feasible. The use of such terminology is then addressed in relation to particular biological issues. The NSOM approach utilizes non-ionizing visible radiation and can be used for non-destructive visualization of active biological structures in air or aqueous settings, with a resolution equivalent to that of scanning electron microscopy.

Most imaging methods currently in use are essentially limited by the radiation's wavelength. In this paper we present our discovery of a specific new method of imaging, independent of the wavelength of the radiation. This method allows the non-destructive imaging of surfaces within their native environment, with a resolution equivalent to the microscopy of electron scans. This breakthrough in biophysical technology has been called "near field optical microscopy scanning" (NSOM). In addition, unlike other methods in this range, near-field imaging would be able to observe the temporal evolution in living cells of these macromolecular assemblies. Hence NSOM has the capacity to provide both kinetic and high spatial resolution information.

## **X. NSOM APPLICATIONS**

### **A. AMPLITUDE AND PHASE CONTRAST**

The release of illumination beam from preparing interactivity region was captured as an effective photo detector for a phase or amplitude comparison picture of a sample.

#### **1. Metal island film**

To illustrate the method a 15 nm thick island of aluminum foil produced using the technique of the latex shadow mask to show its contrasting amplitude. Relevant artifacts are metal patches in the aperture within orbits. Formation is observed by spheres being evaporated and then dissolved.

In order to determine their dimension, we propose choosing as a standard the magnitude equal-sided triangle. The elevation is length  $h = (\sqrt{3}-3/2)d \approx 0.23d$  where  $d$  is the radius of the sphere. Closest adjacent interval within metal trace elements is  $d/\sqrt{3} = 127$  nm.

A measuring interval within traces are on line having the picture of the shear force [Fig. 12.1(b)] Sampling. Illustration of the shear force refers as a involvement on the aperture rim of a very blunt protrusion with real topography of the samples. There is also no apparent triangular structure of metal pieces, this has been SEM-confirmed separately.

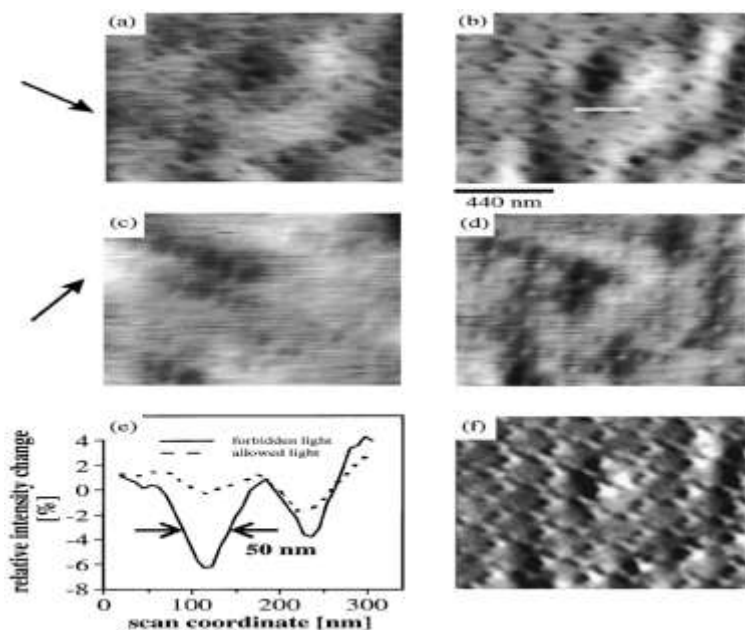


fig12.1

Optical images [Figs.12.1(c) and 12.1(d)] in constant-height mode were observed with the similar peak as the one used for Fig. 12.1(b). The exclusion of illumination of rays are polarized straightly with two orthogonal directions [arrows in Figs.12.1(c) &12.1(d)]. Approximately 15 was the estimated extinction ratio. Fig.12.1(c) by eliminating long-range (far-field) modulations to achieve better visibility of the small structures.

The results from the optical scan [Figs. 12.1(c) and 12.1(d)] have different fine structures. Mentioning the metal patches the hexagonal pattern was well clearly observed.

The structures reveal systemic defects in the optical images. The very sharp double-peak structure is washed out a few nanometers behind the aperture plane, creating an approximately elliptic spot. The direction of the greatest confinement therefore corresponds to the direction perpendicular to the polarization in accordance with the elongation observed.

## 2. *Dielectric scraping*

Stage comparison may be observed during experimental imagery induces optical direction variability. A dielectric grating is one the typical example of that sample. The galvanized structure has a wide thin glass substrate with a length of 383 nm and a phase of 8 nm height.

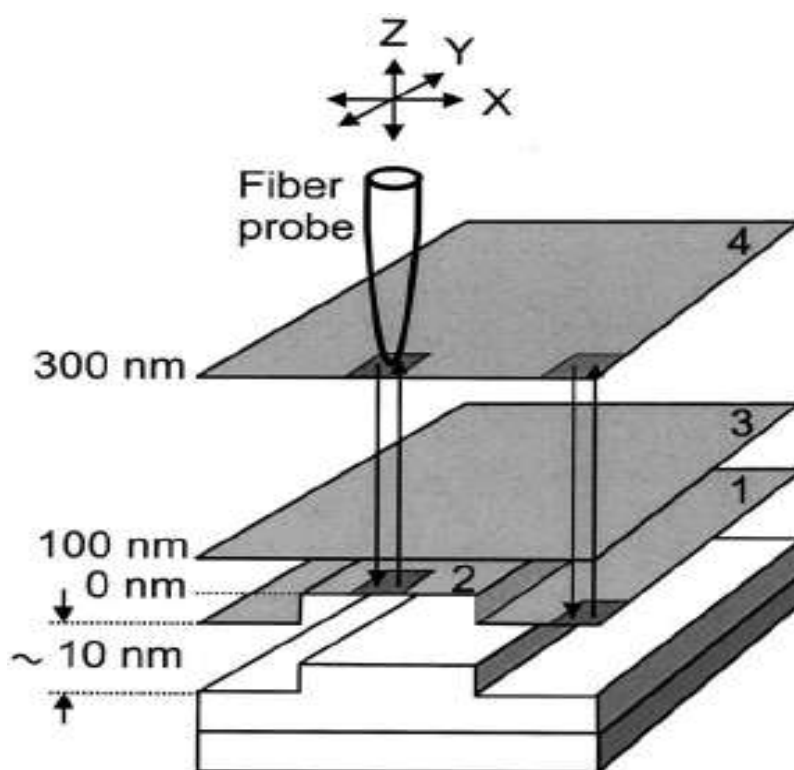


fig 10

Figure 10(c) shows an optical image, captured at a gap width below 1 nm, with a very high resolution constant height mode. Figures 10(d) and 10(e) display optical images captured in the constant height mode with gaps of a few nm and 100 nm, respectively. This collection of photos clearly evidences the resolution's heavy dependency on the gap width..



## ***B. FLUORESCENCE TOMOGRAPHY***

Great vision of picture with fluorescent labeling of living specimen is one of major exciting technology areas for SNOM/NSOM has the ability to imagine the delivery of single fluorophores of the labels.

Surfaces are of concern in biotics and molecular biology, because they expedite prospect of controllable deposition by small quantities of reagents on a scale with nano-meter of well-defined biologically active molecules and chemical assessments.

Micro-contact-printed patches of protein molecules, specifically chicken immunoglobulins, have been investigated. The patches consist of a monolayer,  $4 \times 10 \times 14 \text{ nm}^3$  in size, of closed pack protein molecules.

Each protein molecule is labeled with approximately four dye molecules.

Fluorophores use a single photon diode for avalanche tracking for the purpose of oil immersion. Figure 11(a) displays a picture having two quadrilateral protein traces near-field fluorescence, usually having  $500 \times 3000 \text{ nm}^2$  dimensions

Characterization of these renders the specimen fit as a test of NSOM resolution. Fig. presents a structure's topography of shear force reported at the same time. The sensitivity profiles have been taken from the optical picture to approximate the optical resolution [Figure. 11(a)] identified with lines a or b in two positions.

The wide dimension represents lower element in Fig. allows for a 80 nm resolution. In topographic, crosstalk does not cause a function in the optical picture.

In optical and topographic images, a contrast of the line profiles taken in 11(c) reveals a gap of around 100 nanometres.

This effect occurs frequently at NSOM pictures.

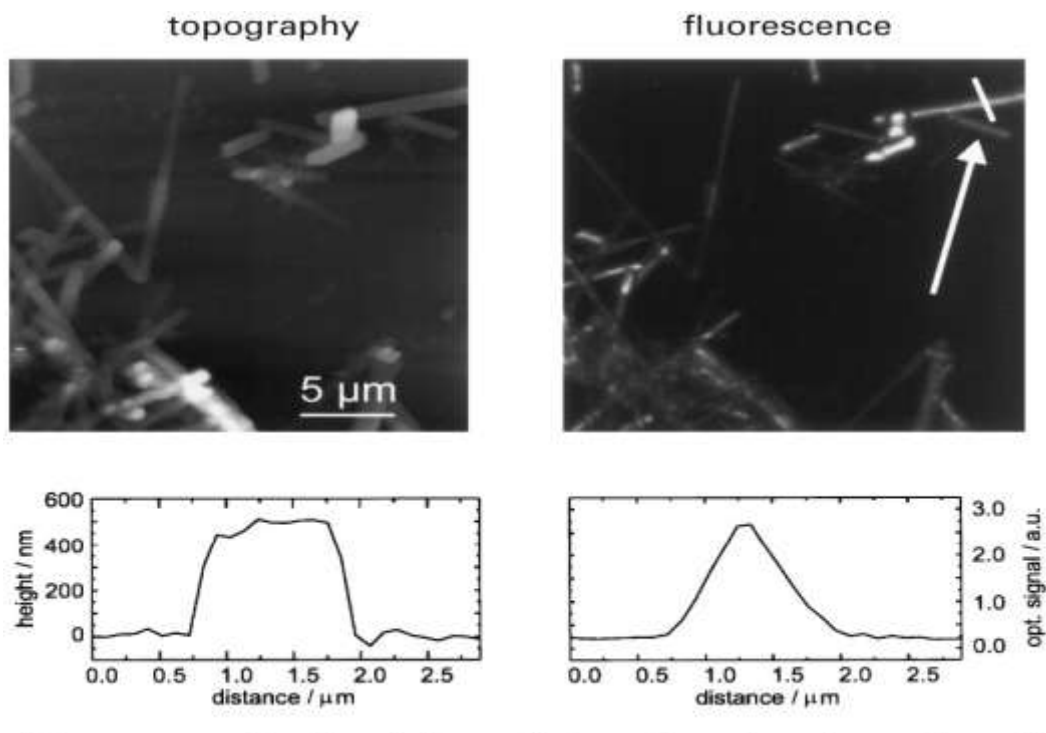


FIG11

(a) High-resolution (512×512 pixel) scanning near-field fluorescence image of a contact-printed pattern of TRITC-labeled chicken immunoglobulin molecules immobilized on a glass surface acquired simultaneously to the shear force image (b). The white arrows (1 and 2) mark the positions where the profiles shown in (c) and (d) were taken. (c) Fluorescence and topography profile along 1, and (d) Fluorescence and topography profile along 2.

Field enhancement and gap-dependent resonance in a system of two opposing tip-to-tip Au nanotriangles Arvind Sundaramurthy et al., *Phys. Rev. B* 72, 165409 (2005)

C. RAMAN SPECTROSCOPIC TECHNIQUE AT NEAR FIELD

Near-field optics at conjunction having resonating resolutions may produce contrast with mentioning dimensions of probe technique. The major issues with the usage of this technique combination are Raman scattering's poor performance and lack of sufficient fiber quality IR spectrum.

The usage of new, noble metal substrate is an ability to increase the broad cross section of Raman to display signals in SNOMs.

The impact of improved surface in signals observed may surpass many metal features' morphology and shape. There is still some controversy regarding the cause for the heavy enhancement.

There are reasons to use two separate processes.

Because of the raw topography of the substratum, it is essential that the sample itself differentiates between the contrast caused topographically and changes in the strength due to substratum absorption.

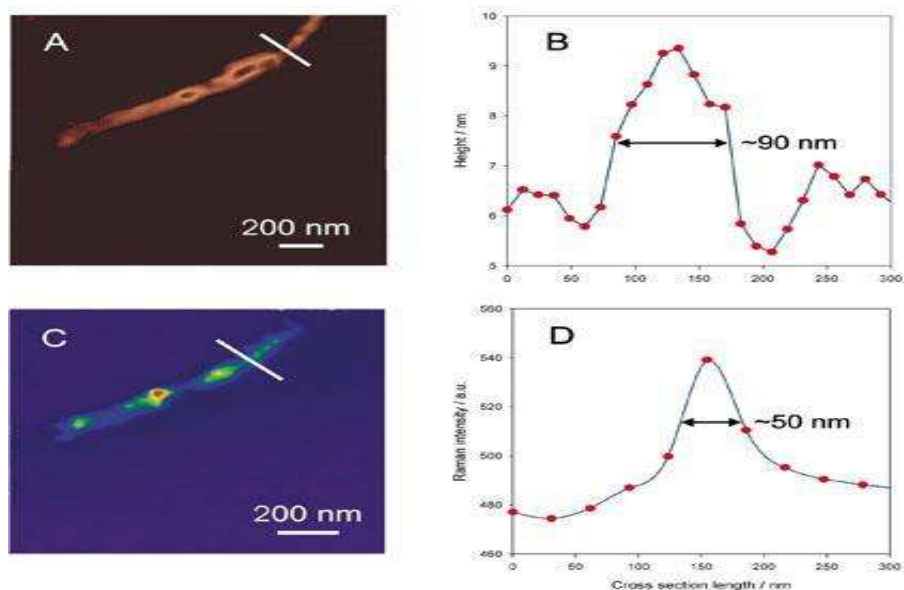
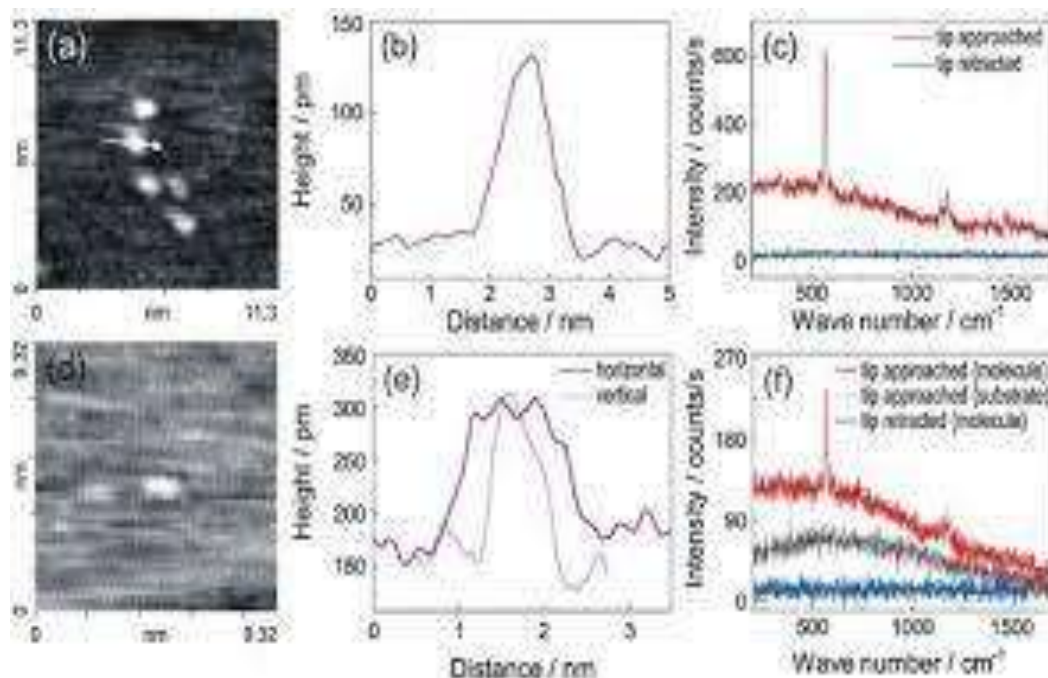


fig13



These pair of pictures ... Figs. 13(b) and 13(d), recorded as placing on various Raman bands, display very several characteristics. Figure 13(b) reported on a near-field probe Raman glass band, whereas Fig. 13(d) corresponds to a named Raman DNA signal. The 13(b) signals composite to a Raman labeled DNA signal. The 13(b) signals show the silver sphere layer reflectivity (absorption). Of note, a higher sample reflectivity often concludes in an improvement in the observed Raman intensity.

Situation regarding Raman magnifies surface collecting strengths of the signal may consist of very large frequency.

Additionally, the identification of a few hundred molecules was seen for NFO experiments. Thus the system appears to obtain the capacity having particle identification over lateral calibration.

Figure 13.1 contrasts the xylene nearfield and Raman farfield spectra.

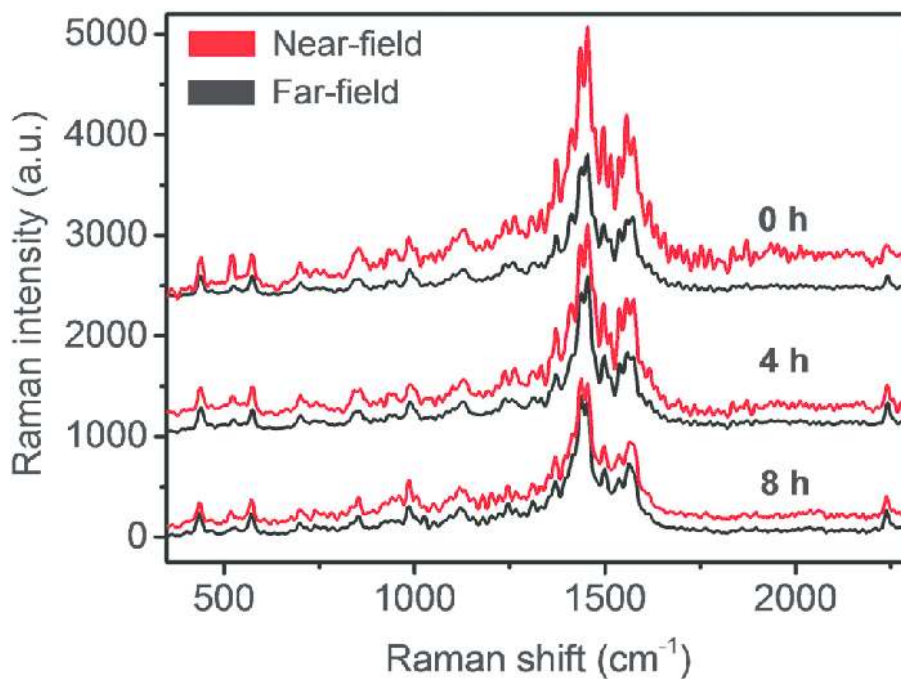


fig13.1

### Terahertz near-field measurements

Various methods from a visible to a THz frequency system are used for near-field imaging with a spatial resolution of sub wavelengths.

The usage of a void opening in a metal is one method for increasing spatial resolution.

In 1998 the first THz example with a spatial resolution of  $\mu/4$ , as shown in Fig. 13.2,

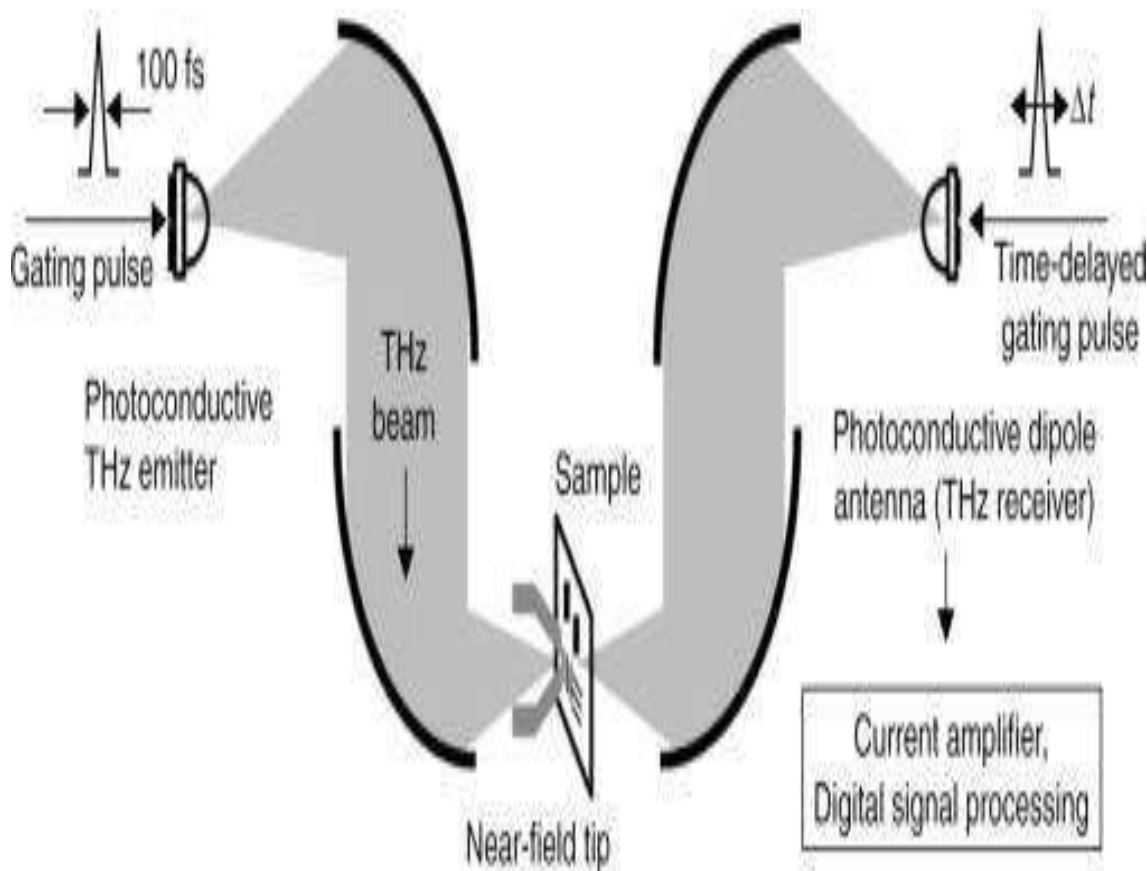


Fig 13.2

The close field measurement process, Optical Microscopy Near Field Scanning (ASNOM), is designed to disperse light via a metal spike of sub-wavelengths.

Rates of THz may be purely based on the pointed peak of copper.

The agonizing tip of the copper wire and tincture magnitude of electric field THz locally situated.

The local vector has been expanded or enlarged by scanning close-field microscopy (CFR microscopy).

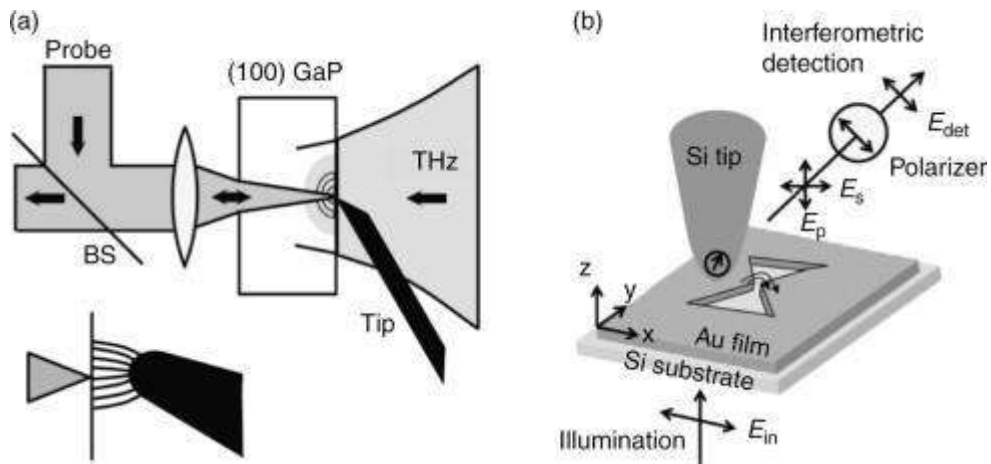


Fig 13.4

Both aperture and open case provide a spatial range based on the opening or curvature of the extremity radius. The signal descends as  $a^6/\alpha^4$  to the radius opening  $a$ , which restricts its performance.

This approach has the advantage of demonstrating growth of narrow to wider areas.

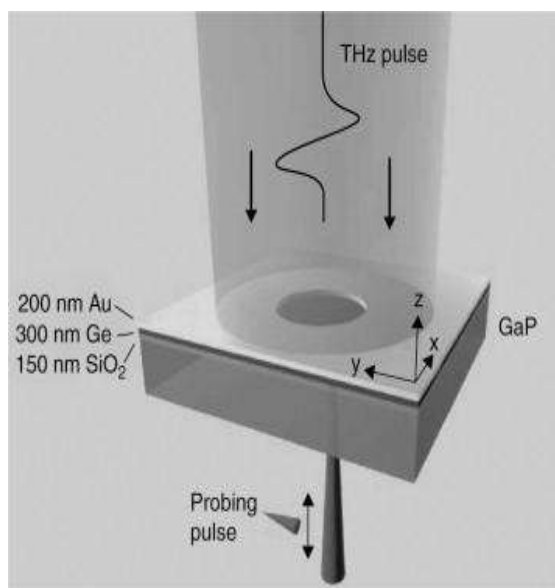


fig13.5

The birefringence induces a polarization difference in the pulse passing from crystal for estimation of EO.

Through estimation of the energy gap in 2 Wollaston prism and two photodiodes orthogonal polarization direction beams a light equal to the electrical field of THz.

The EO detection is generally focused on zinc blending crystals such as ZnTe and Void. By choosing the crystal detector direction, you may choose the component that is prone to EO detector in the electric vector THz.

From calculation having triple compounds with electrical field as after shifting can also be determined via the Maxwell equations,

$$\nabla \times \mathbf{E} = -\frac{\partial \mathbf{B}}{\partial t}$$

Fig 14 displays THz electrical near-field vectors estimated length having five hundred nanometers.

The negative and positive amplitudes are shown by black and white in the magnetic field. This process approach has been used both in THz and infrared.



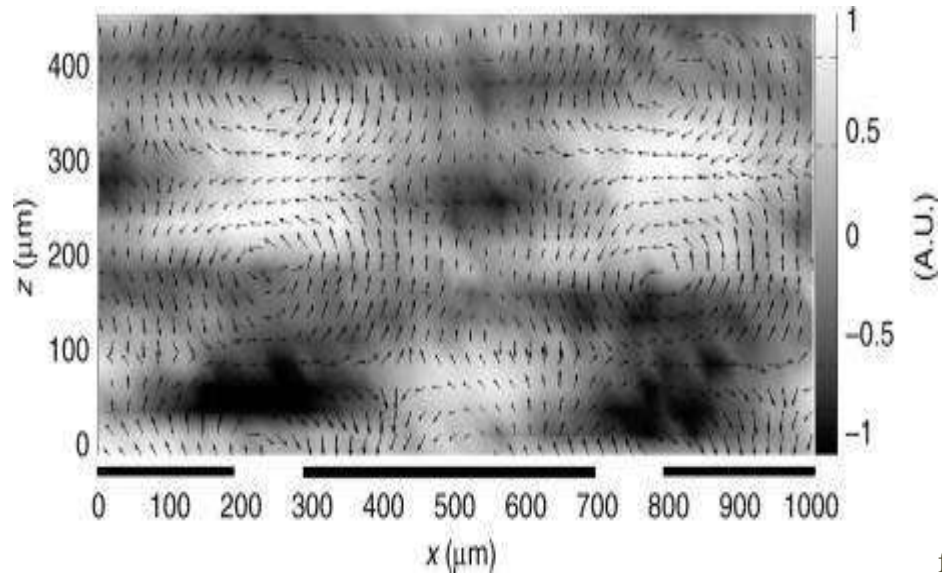


fig14

Here we concentrate principally on the EO sampling technique.

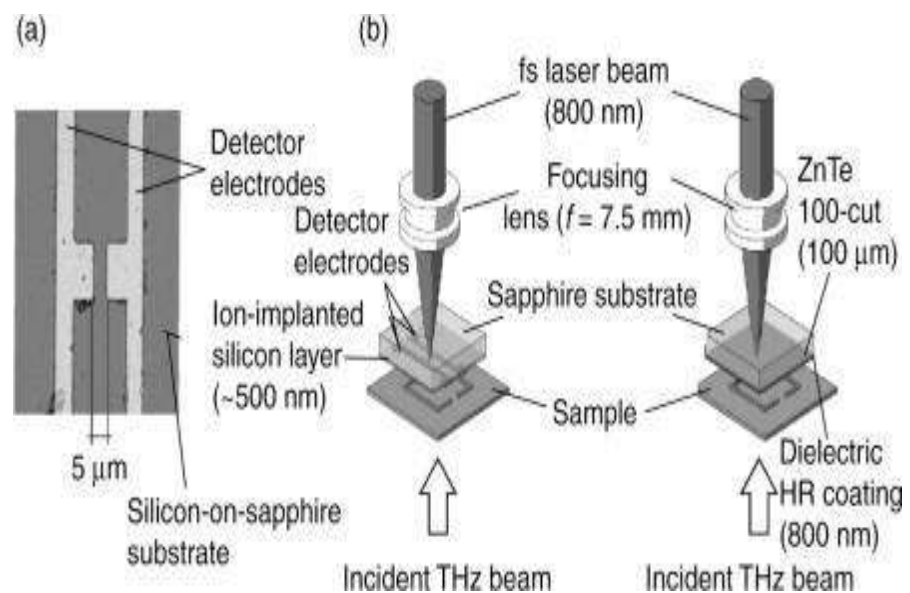


fig14.7a,b

#### *D. PULSED LASER ABLATION THROUGH NSOM TIPS*

The tube etching scanning probe samples will survive a few ten milliJoule and they are sufficiently stable.

The aperture strength may exceed  $10^8 \text{ W / cm}^2$ , that might be sufficient for preparation near the tip from being removed. Various functions for laser-persuade erosion/ablation is possible via NSOM tips. The light insulated chemical model indicates absorption through electrical absorption into the sample and the ablation happens due to the disintegration of chemical bonds.

Similarly, the absorbed optical energy will be transformed into heat in a photothermal situation, causing the locally heated spot to ablaze. Second, a ballistic mechanism is possible, where water sprinkled over preparations from the tip, leading the substance to be separated from its surface.

Fourthly, the transient thermal expansion must also be taken into account as a potential mechanism for producing surface indentations.

We are now debating a test which described specific progress from a rhodamine B film about the ablation mechanism.

Figures 15(b) and 15(c) display topographic images of shear force that were reported exceeding many rays of frequencies(pulses) has been observed

[Fig.15(b),  $\lambda = 650 \text{ nm}$ , pulsating energy of  $2.1 \mu\text{J}$ ]. In comparison, with the sample highly absorbs [Fig.]. 15(c),  $\lambda = 532 \text{ nm}$ , pulsed energy of  $1.4 \mu\text{J}$ . Energy transfer through photon absorption seems more effective than through a ballistic cycle.

Accordingly, we propose that a thermal insulation mechanism is in charge having ablation by Rh coating.

Giving opinion for photon energy intake and transforming into resonating excitement which leads to a rapid increase in temperature causing molecular insulation.

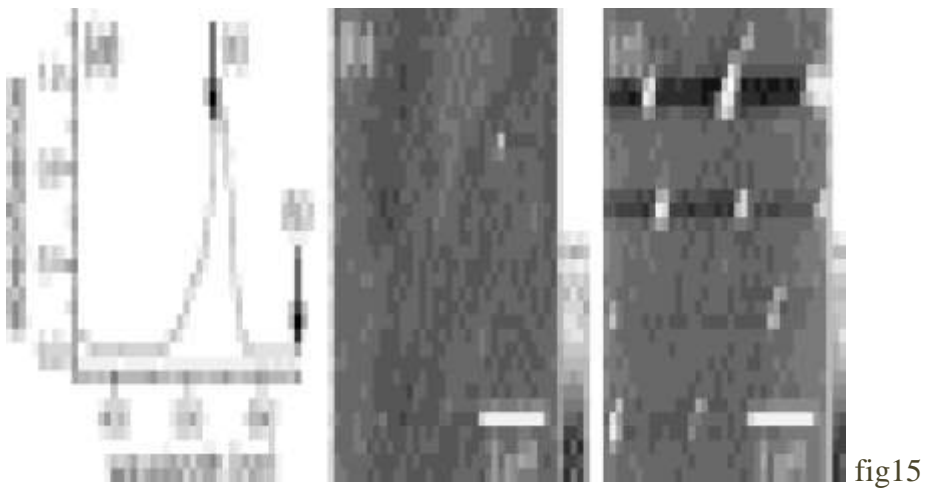


Fig. 15(c) represents redeposits the ablated material on the surface of the sample near to the ablation crater.

In this experiment, it was not a symmetrical distribution of the redeposited content can be proved by this experiment.

## **XI. PERSPECTIVES**

Viewing this review, we concentrate on the basics and chosen implementation of aperture NSOM and only fulfill the limited proportion from its work ongoing in the field of NFO. The reader is directed to other NFO analysis papers and recent reviews for a more full image in this issue. The rapid growth of NFO techniques is far from over.

There are still many issues to be overcome and many diligent studies yet to be performed. The technological question of tip growth, in particular in terms of tip stability, dangerous threshold and transmission coefficients, still needs to be strengthened.

Microfabricated near-field samples can contribute to solving these problems by providing better defined experimental and reproductive conditions.

Often helpful are modern tip ideas that deviate from the traditional opening scheme. A cut-off region by the tapering areas should travel towards the top, thereby rising the transmission coefficient considerably. Usage of smaller apertures will exploit this. Additionally, instead of using fluorescent markers, direct excitation of some biomolecules may become feasible.

Moreover, the use of UV excitement is advantageous in Raman spectroscopy, due to the 4-dependent disperse efficiency and the capacity for the increase of small silver particles in the resonant field in that spectral region.

Aperture less contraction for fluorescence imaging, is one of the most promising candidates for major resolution enhancement.

We also haven't discussed all the many new structures of contrast that are constantly developing. We haven't listed, for example, time-resolved SNOM, which combines optical resolution of the nanometer scale with resolution of the femtosecond time. In this field a variety of groups already function.

According to our knowledge and information, the NSOM region can be incredibly beneficial with modeling and experimental interactions.

This partnership, however, has not yet been as successful as one wishes. This could be because of the limitations intrinsic to a realistic laboratory set up (even top, sample and detection) of computational virtual simulations and vice versa because of laboratory difficulties in correctly measuring the required parameters.

In actual, for instance, our simulations are seen in the Fig. 8,

To be able to equate the experimentalists with theoretical models, one should hope for the future.

On contrarily side, ideologue theorizer should increase its calculating equations capacity. Such relationships should be of help to all parties.

## REFERENCES

1. C. Girard and A. Dereux, *Rep. Prog. Phys.* **59**, 657 (1996). [[Inspec](#)] [[ISI](#)] [[ChemPort](#)] [first citation in article](#).
2. D. Pohl, W. Denk, and M. Lanz, *Appl. Phys. Lett.* **44**, 651 (1984). [First Citation in article](#)
3. U. Dürig, D. Pohl, and F. Rohner, *J. Appl. Phys.* **59**, 3318 (1986). [[ISI](#)] [First citation in article](#)
4. E. Betzig, M. Isaacson, and A. Lewis, *Appl. Phys. Lett.* **51**, 2088 (1987). [[ISI](#)] [first citation in article](#)
5. G. Binnig and H. Rohrer, *Helv. Phys. Acta* **55**, 726 (1982). [[Inspec](#)] [[ChemPort](#)] [first citation in article](#)
6. J. Koglin, U. Fischer, and H. Fuchs, *J. Biomed. Opt.* **1**, 75 (1996). [First Citation in article](#).
7. M. Abbé, *Archiv. Microscope. Anat. Entwickl lungsmech.* **9**, 413 (1873). [First citation in article](#)
8. *Near Field Optics and Related Techniques, Ultramicroscopy*, Vol. 61, edited by P. Kruit, M. Paesler, and N. van Hulst (North Holland, Elsevier, Amsterdam, 1995), Proceeding of NFO III, Brno, Czech Republic, 9–11 May 1995. [first citation in article](#)
9. *Proceedings NFO-5, J. Microscopy*, Vol. 194, edited by S. Kawata (Blackwell Science Ltd., Oxford, 1999), Proceeding of NFO 5, Shirahama, Japan, 6–10 December 1998. [first citation in article](#)
10. J. W. Goodman, *Introduction to Fourier Optics, Physical and Quantum Electronics Series* (McGraw-Hill, New York, 1968). [first citation in article](#)
11. M. Abbé, *Archiv. Mikroskop. Anat. Entwicklungsmech.* **9**, 413 (1873). [first citation in article](#)
12. T. Wilson and C. J. R. Sheppard, *Theory and Practice of Scanning Optical Microscopy* (Academic, London, 1984). [first citation in article](#)
13. *Handbook of Biological Confocal Microscopy*, edited by J. Pawley (Plenum, New York, 1995). [first citation in article](#)
14. E. Synge, *Philos. Mag.* **6**, 356 (1928). [[ChemPort](#)] [first citation in article](#)

15. E. Synge, *Philos. Mag.* 11, 65 (1931). [first citation in article](#)
16. H. Heinzelmann, B. Hecht, L. Novotny, and D. Pohl, *J. Microsc.* 177, 115 (1994). [\[Inspec\]](#) [\[ISI\]](#) [first citation in article](#)
17. B. Hecht, H. Heinzelmann, and D. Pohl, *Ultramicroscopy* 57, 228 (1995). [\[Inspec\]](#) [\[ISI\]](#) [\[ChemPort\]](#) [first citation in article](#)
18. U. Fischer and D. Pohl, *Phys. Rev. Lett.* 62, 458 (1989). [\[ISI\]](#) [\[MEDLINE\]](#) [\[ChemPort\]](#) [first citation in article](#)
19. F. Zenhausern, Y. Martin, and H. Wickramasinghe, *Science* 269, 1083 (1995). [\[Inspec\]](#) [\[ISI\]](#) [\[ChemPort\]](#) [first citation in article](#)
20. Y. Inouye and S. Kawata, *J. Microsc.* 178, 14 (1995). [\[Inspec\]](#) [\[ISI\]](#) [first citation in article](#)
21. P. Gleyzes, A. Boccara, and R. Bachelot, *Ultramicroscopy* 57, 318 (1995). [\[Inspec\]](#) [\[ISI\]](#) [\[ChemPort\]](#) [first citation in article](#)
22. N. van Hulst, M. Moers, and E. Borgonjen, *NATO Series E: "Photons and Local Probes,"* edited by O. Marti and R. Möller (Kluwer Academic, Dordrecht, 1995), Vol. E 300, p. 165. [first citation in article](#)
22. R. Toledo-Crow, P. Yang, Y. Chen, and M. Vaez-Iravani, *Appl. Phys. Lett.* 60, 2957 (1992). [\[ISI\]](#) [\[ChemPort\]](#) [first citation in article](#)
23. E. Betzig, P. Finn, and S. Weiner, *Appl. Phys. Lett.* 60, 2484 (1992). [\[ISI\]](#) [\[ChemPort\]](#) [first citation in article](#)
24. K. Karrai and R. Grober, *Appl. Phys. Lett.* 66, 1842 (1995). [\[ISI\]](#) [\[ChemPort\]](#) [first citation in article](#)
25. B. Hecht, *Forbidden Light Scanning Near-Field Optical Microscopy*, Ph.D. thesis, University of Basel (Hartung-Gorre, ISBN 3-89649-072-9, Konstanz, 1996). [first citation in article](#)
26. G. Tarrach, M. Bopp, D. Zeisel, and A. Meixner, *Rev. Sci. Instrum.* 66, 3569 (1995). [\[ISI\]](#) [\[ChemPort\]](#) [first citation in article](#)
27. M. Pfeffer, P. Lambelet, and F. Marquis-Weible, *Rev. Sci. Instrum.* 68, 4478 (1997). [\[ISI\]](#) [\[ChemPort\]](#) [first citation in article](#)
28. T. Okajima and S. Hirotsu, *Appl. Phys. Lett.* 71, 545 (1997). [\[ISI\]](#) [\[ChemPort\]](#) [first citation in article](#)
29. S. Davy, M. Spajer, and D. Coujon, *Appl. Phys. Lett.* 73, 2594 (1998).

[ISI] [ChemPort] first citation in article

30. M. Gregor, P. Blome, J. Schöfer, and R. Ulbrich, *Appl. Phys. Lett.* 68, 307 (1996). [ISI] [ChemPort] first citation in article

31. H. Bielefeldt, Ph.D. thesis, University of Konstanz, 1994. first citation in article.

32. <https://www.sciencedirect.com/topics/chemistry/scanning-near-field-optical-microscopy>

33. H. W. Deckman and J. H. Dunsmuir, *Appl. Phys. Lett.* 41, 377 (1982). [ISI] [ChemPort] first citation in article

34. L. Novotny and D. Pohl, in Ref. 40, Vol. 300, p. 21. first citation in article

35. L. Novotny, D. W. Pohl, and B. Hecht, *Ultramicroscopy* 61, 1 (1995). [Inspec] [ISI] [ChemPort] first citation in article

36. M. Garcia-Parajo et al., *Bioimaging* 6, 43 (1998). [Inspec] [ChemPort] first citation in article

37. N. van Hulst, *J. Chem. Phys.* 112, 7799 (2000), this issue. [ISI] [ChemPort] first citation in article

38. A. Bernard et al., *Langmuir* 14, 2225 (1998). [Inspec] [ISI] [ChemPort] first citation in article

39. T. Schmidt, G. Schütz, H. Gruber, and H. Schindler, *Anal. Chem.* 68, 4397 (1996). [ISI] [ChemPort] first citation in article

40. W. Trapesinger et al., *Anal. Chem.* 71, 279 (1999). [ISI] [MEDLINE] [ChemPort] first citation in article

41. D. A. Smith et al., *Ultramicroscopy* 61, 247 (1995). [Inspec] [ISI] [ChemPort] first citation in article

42. C. L. Jahncke, H. D. Hallen, and M. A. Paesler, *J. Raman Spectrosc.* 27, 579 (1996). [Inspec] [ISI] [ChemPort] first citation in article

43. D. Zeisel et al., *Anal. Chem.* 69, 749 (1997). [ISI] [ChemPort] first citation in article

44. S. Nishikawa and T. Isu, *J. Microsc.* 194, 15 (1999). first citation in article

45. A. Kramer et al., *Biophys. J.* 78, 458 (2000). [Inspec] [ISI] [MEDLINE] [ChemPort] first citation in article



46. H. Metiu, *Prog. Surf. Sci.* 17, 153 (1984). [Inspec] [ChemPort] first citation in article
47. Y. Kawata, C. Xu, and W. Denk, *J. Appl. Phys.* 85, 1294 (1999). [ISI] [ChemPort] first citation in article
48. V. L. S. K. Sekatskii, *Appl. Phys. B: Lasers Opt.* 63, 525 (1996). [Inspec] [ISI] first citation in article
49. V. L. S. K. Sekatskii, *JETP Lett.* 65, 465 (1997). [ISI] first citation in article

## Thesis

### ORIGINALITY REPORT

3%

SIMILARITY INDEX

1%

INTERNET SOURCES

3%

PUBLICATIONS

1%

STUDENT PAPERS

### PRIMARY SOURCES

1

Bert Hecht. "Scanning near-field optical microscopy with aperture probes: Fundamentals and applications", The Journal of Chemical Physics, 2000

Publication

1%

2

Fu-Ren F. Fan, Biao Liu, Janine Mauzeroll. "Scanning Electrochemical Microscopy", Elsevier BV, 2007

Publication

1%

3

[www.nanoscale-optics.de](http://www.nanoscale-optics.de)

Internet Source

1%

4

Bernhard Knoll, Fritz Keilmann. "Enhanced dielectric contrast in scattering-type scanning near-field optical microscopy", Optics Communications, 2000

Publication

<1%

Exclude quotes

On

Exclude matches

< 15 words

Exclude bibliography

Off